

Stark broadening in krypton and xenon

A. Lesage and D. Abadie

Observatoire de Paris, Section d'Astrophysique de Meudon, 92195 Meudon CEDEX, France

M. H. Miller

Department of Mechanical Engineering, U.S. Naval Academy, Annapolis, Maryland 21402

(Received 17 October 1988)

Broadening of visible Kr I, Kr II, and Xe II lines is measured behind reflected shock waves in a diaphragm shock tube. Revised estimates of broadening by competing mechanisms reduce the Stark parameters for seven lines of Xe II measured earlier in the shock tube. Stark broadening for 30 lines are obtained, including 16 not previously reported. Results are compared with findings elsewhere, and systematic broadening trends in the homologous ion sequence are examined.

I. INTRODUCTION

Systematic trends are often found in the Stark broadening of strong emission lines.¹ For prominent visible lines of homologous ions, such trends can persist over four rows of the Periodic Table.² Recent measurements of Kr II and Xe II widths have sought to determine the effects pronounced fine-structure splitting have on systematic Stark-broadening trends³⁻⁶

The present shock-tube experiments were intended to simultaneously record Ar II, Kr II, and Xe II visible line profiles and then compare the measured widths in an attempt to evaluate trends and to discover possible sources of discrepancy between data from past shock-tube experiments⁶ and from other light sources.⁵ In particular, we wanted to find out if Stark broadening in the heavy rare-gas ions varies approximately linearly with the principal quantum number n , as had been suggested by comparison with line broadening in the "mirror-image" alkaline earth ions.⁶ Furthermore, such measurements help determine whether array-averaged semiempirical (SE) computations,⁷ which successfully approximate the comparative Stark broadening of third-period ionic lines⁸ are still of use in the presence of pronounced fine-structure splitting.

II. EXPERIMENT

The apparatus and methods have been described previously,^{6,8,9} but the gas compositions are new, consisting of neon as carrier gas and an admixture of either 1.97% Ar + 1.05% Kr + 0.63% Xe, or 0.20% SiH₄ + 0.57 Kr, or 0.68% B₂H₆ + 7.9% Kr (partial pressures). In the test section, filling pressures are in the 15–30-Torr range. The bursting pressures in the driver section are 80–100 atm. The shock-compressed and -heated plasma behind the first and multiply reflected shock waves is in the 7–12-atm and 10 000–12 000-K ranges. The corresponding electron densities, determined by fitting H_{β} profiles to the theoretical Stark shapes,¹⁰ range from 5 to 20×10^{16} cm⁻³. In some electron-density determinations, empirical corrections¹¹ have been reported to the theoretical

widths.¹⁰ On the average, these corrections increased the measured electron density by 3%.

Various combinations of initial conditions and photographic exposure times were tried in an effort to obtain good photographic image densities for the simultaneously recorded Ar II, Kr II, and Xe II lines, but the argon-ion lines were always too faint. Simultaneous recording of Kr II and Xe II was frequently possible, though.

The improved photometric quality of some of the later experiments revealed that we had sometimes undercompensated for finite optical depths in our earlier experiments. For the brighter Xe II lines, the proper compensation is a 2–7% reduction in the line profile widths.

The Lorentzian components of the measured widths were reduced in the usual way.¹² The Lorentzian linewidths were $1\frac{1}{2}$ –2 times the width of the instrument profile, which was Gaussian. Collisions with neon atoms at shock-tube pressures of 10 atm can cause van der Waals broadening by some 0.1 Å (Ref. 13) for the typical Kr II and Xe II lines. This effect had been neglected earlier,⁶ but here we used Griem's formulas¹³ to correct for this competing broadening. Most data were collected within ± 500 K of 11 000 K and no attempt was made to normalize to one temperature.

III. RESULTS AND DISCUSSION

The experimental Stark widths and electron densities N_e are shown in Fig. 1 for typical 6s-6p and 6p-6d Xe II and 5s-5p Kr II lines. Our random error estimates are based on the grain noise in our fast emulsions and on the reading errors in determining the baselines of the investigated lines and H_{β} profiles. To within experimental accuracy, the broadening is linear in electron density for both the narrower and wider investigated lines.

The data points in Fig. 2 are for Xe II and Kr II Stark profiles of lines simultaneously recorded on the same exposures. These data are linearly related. The slope agrees with the corresponding linewidth ratio determined from Kr II (Ref. 14) and Xe II (Ref. 5) data from cascade arc experiments.

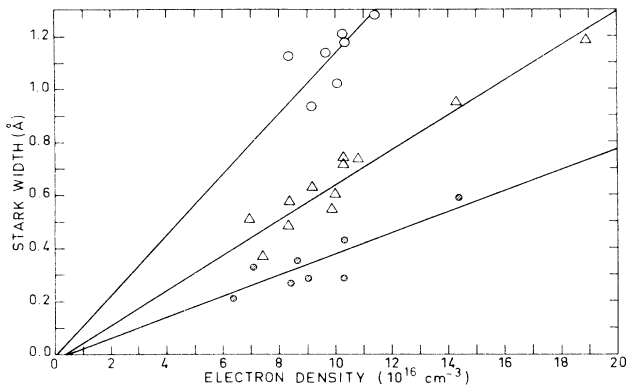


FIG. 1. Measured broadening of Xe II lines at 4238.3 Å ($6p-6d$) and Xe II lines at 4603.0 Å ($6s-6p$), and the Kr II line at 4355.5 Å ($5s-5p$) vs electron density. Widths are FWHM, corrected for instrumental and van der Waals broadening, but including broadening by ions. The Xe II lines 4238.3 and 4603.0 Å are denoted by open circles and triangles, respectively, and the Kr II line at 4355.5 Å is denoted by shaded circles.

The present results and experimental comparisons for Kr I and Kr II are given in Table I, and for Xe II in Table II. The estimated error in the broadening parameters is 25%. The random errors in the broadening parameter averages (from four to 15 experiments per line) are usually 10–17%, due mainly to grain noise, interference, and profile baseline fitting. Transient spatial inhomogeneities and temporal fluctuations during exposure contribute to jitter but do not invalidate the results because (i) the investigated lines and H_{β} tend to react covariantly to small source fluctuations, and (ii) large fluctuations in excitation temperature are detected by monitoring the photoelectric intensity of the Ne I line at 5852 Å, while large electron-density deviations are detected photoelectrically

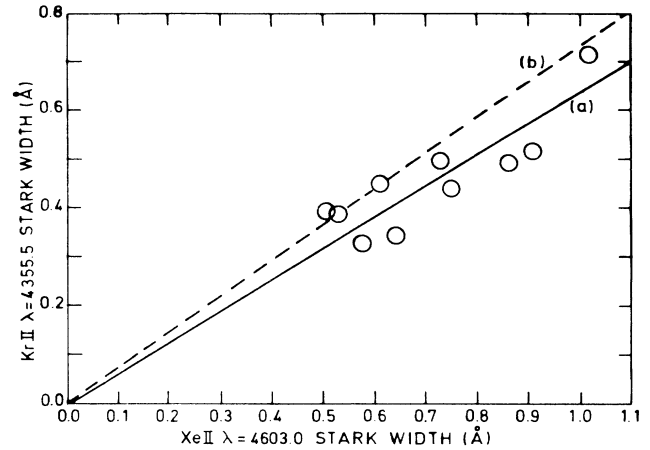


FIG. 2. Comparison of Kr II and Xe II Stark widths from simultaneously recorded line profiles. Line *a* denotes the ratio adopted (including data recorded in experiments where the lines appear separately), and line *b* indicates the corresponding ratio of the data Nick *et al.* (Ref. 5) to that of Brandt *et al.* (Ref. 14).

as shifts in the continuum (whose intensity scales as N_e^2). When large temporal fluctuations occur, usually because a shock transition zone is inadvertently sampled, the data are discarded.

There are several possible sources of reproducible error: (i) Uncertainty in the computed approximations of the van der Waals widths contributes 5–8% (that is, 50% uncertainty in a 10–16% correction term), (ii) slight undetected densitometer-slit misalignments can increase linewidths in a single experiment by a few percent. The reproducible errors in slit deconvolution and in optical-depth compensation should each average less than 5%.

For the one Kr I line where measurements overlap, Table I shows that the present results are 30% larger

TABLE I. Experimental Stark half-widths [full width at half maximum (FWHM)] for krypton (in Å) for an electron density of 10^{17} cm^{-3} and a mean temperature of 11 000 K.

Spectrum	Transition ^a	Wavelength (Å)	This work	Klein <i>et al.</i> ^b	Brandt <i>et al.</i> ^c
Kr I	$5s(\frac{3}{2})_2 - 6p(\frac{3}{2})_2$	4274.0	2.75 ^d		
	$5s(\frac{3}{2})_1 - 6p(\frac{3}{2})_1$	4463.7	2.63 ^d		
	$5s(\frac{3}{2})_2 - 5p'(\frac{1}{2})_1$	5570.3	0.86 ^d	0.96 ^e	0.63
Kr II	$5s^4P_{5/2} - 5p^4D_{7/2}^o$	4355.5	0.39 ^f		
	$5s^4P_{3/2} - 5p^4D_{5/2}^o$	4765.7	0.51 ^f		0.39
	$5s^4P_{5/2} - 5p^4D_{3/2}^o$	4739.0	0.49 ^f		0.29
	$5s^4P_{3/2} - 5p^4D_{3/2}^o$	4292.9	0.30 ^f		
	$5s^4P_{1/2} - 5p^4D_{1/2}^o$	4431.7	0.31 ^f		
	$5s^4P_{5/2} - 5p^4P_{3/2}^o$	4658.9	0.45 ^f		
	$5s^2P_{3/2} - 5p^2D_{3/2}^o$	4619.2	0.54 ^f		0.34

^aReference 16.

^bReference 15.

^cReference 14.

^dEstimated accuracy $\pm 20\%$.

^eTemperatures $(9.4-10.3) \times 10^4 \text{ K}$.

^fEstimated accuracy $\pm 25\%$.

than the Stark widths from a cascade arc¹⁴ and are 10% smaller than those from another shock-tube experiment.¹⁵ The present Kr II widths exceed those of Brand *et al.*¹⁴ by 30–70%, thereby going beyond the estimated combined tolerances. Electron densities and temperatures in the two experiments are comparable. Total densities in the two experiments differ by an order of magnitude, but van der Waals widths are compensated for the same way in both experiments.

The measured and adjusted Stark widths for Xe II are given in Table II. According to our revised analysis, some Xe II widths are reduced by 15–25% from our previous values⁶ and now agree with those of Richou *et al.*⁴ These authors also used a diaphragm-type shock tube, but an optical multichannel analyzer (OMA) II for recording xenon profiles, and they determined electron densities by interferometry rather than by fitting H_{β} profiles. The present results differ from widths measured with a cascade arc⁵ by factors ranging from 0.98 to 1.93. The arc apparatus is appropriate for signal averaging and long test times that reduce random error and, hence, allows the use of narrow slits that avoid systematic deconvolution errors. It also has a tenfold-higher degree of ionization, which causes less of the competing pressure

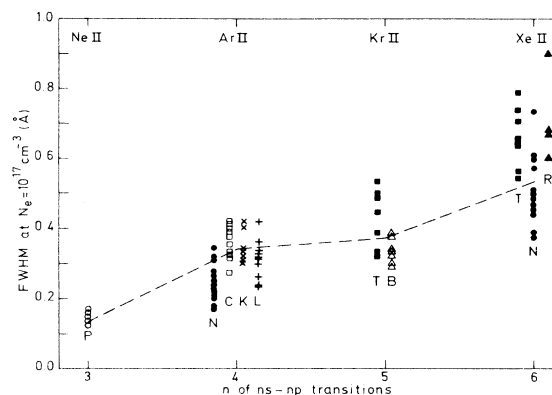


FIG. 3. Comparison of measured Stark half-widths for $ns-np$ transitions in rare-gas first ions. Each point represents an individual line in the transition array. Sources are as follows: *P*, Platasa *et al.* (Ref. 17); *N*, Nick *et al.* (Ref. 5); *C*, Chapelle *et al.* (Ref. 18); *K*, Konjevic *et al.* (Ref. 19); *L*, Labat *et al.* (Ref. 20); *B*, Brandt *et al.* (Ref. 14); *R*, Richou *et al.* (Ref. 4); and *T*, this work. The dashed line connects array-averaged broadening predictions in the semiempirical approximation of Griem (Ref. 7).

TABLE II. Experimental Stark half-widths (FWHM) for Xe II (in Å) for an electron density of 10^{17} cm^{-3} and a temperature of 11 000 K.

Transition ^a	Wavelength (Å)	This work ^b	Prior result ^d	Richou <i>et al.</i> ^c	Nick <i>et al.</i> ^f
$6s^4P_{5/2} - 6p^4D_{7/2}^{\circ}$	4844.3	0.72	0.86		0.383 ^g
$6s^4P_{3/2} - 6p^4D_{5/2}^{\circ}$	5419.1	N.A.	0.95	0.90	0.574 ^g
$6s^4P_{3/2} - 6p^4D_{3/2}^{\circ}$	4603.0	0.65	0.84		0.451 ^g
$6s^4P_{5/2} - 6p^4P_{5/2}^{\circ}$	5292.1	0.79	0.93		0.443 ^g
$6s^4P_{5/2} - 6p^4P_{3/2}^{\circ}$	5339.4	0.64 ^c		0.60	
$6s^4P_{3/2} - 6p^4P_{1/2}^{\circ}$	5372.4	0.65	0.90	0.67	0.495 ^g
$5d^4D_{7/2} - 6p^4D_{7/2}^{\circ}$	5472.6	0.82	0.96		0.596 ^g
$5d^4D_{7/2} - 6p^4D_{5/2}^{\circ}$	5531.1	0.63			
$5d^4D_{5/2} - 6p^4P_{5/2}^{\circ}$	6036.2	0.75			0.658 ^g
$5d^4D_{7/2} - 6p^4P_{5/2}^{\circ}$	6051.1	0.75	0.96		0.686 ^g
$5d^4D_{3/2} - 6p^4P_{1/2}^{\circ}$	5667.6	0.61			0.626 ^g
$6s^2P_{3/2} - 6p^2P_{5/2}^{\circ}$	4921.5	0.56			
$6s^4P_{1/2} - 6p^2P_{3/2}^{\circ}$	4524.2	0.74			
$6s^2P_{3/2} - 6p^2S_{1/2}^{\circ}$	5439.0	0.54		0.67	0.483 ^g
$6s^2D_{5/2} - 6p^2F_{7/2}^{\circ}$	4532.5	0.55			
$5d^2D_{5/2} - 6p^2D_{5/2}^{\circ}$	4414.8	0.44			
$6p^4D_{7/2} - 6d^4D_{7/2}$	4585.5	1.32			
$6p^4P_{3/2} - 6d^4D_{3/2}$	4180.1	1.16			
$6p^4D_{5/2} - 6d^4F_{7/2}$	4330.5	1.32			
no classification	4448.1	1.32			

^aReference 16.

^bEstimated accuracy $\pm 25\%$; lines at 5419.1 subject to interference.

^cUnresolved blend of two Xe II lines (Ref. 16), of which $6s-6p$ should be the strongest.

^dReference 6.

^eReference 4.

^fReference 5.

^gCorrected for Doppler and instrumental broadening, but not corrected for van der Waals broadening (Ref. 5).

broadening than with the shock tube. All these factors suggest that shock-tube error is the source of the present discrepancy. However, with essentially the same apparatus and techniques, the present shock tube has been used to measure Stark widths of other spectra, including C I lines and such narrow lines as those of S II,⁸ in agreement with results from another cascade arc.¹⁶

A recent low-pressure pulsed-arc study of broadening trends for rare-gas-ion np - nd transitions³ included no Xe II line overlap with the present set of data. The measured widths of two $6p^2P^{\circ}$ - $6d^2D$ lines (normalized to $N_e = 10^{17} \text{ cm}^{-3}$) were 1.47 and 1.53 Å, which are not unlike the present widths of 1.14 and 1.32 Å for lines in the $6p^4P^{\circ}$ - $6d^4D$ multiplet.

Experimental Stark-broadening data for ns - np transitions in rare-gas ions are shown in Fig. 3. Regardless of how one weighs the results from a particular study or by a particular method, the trend line is nonlinear in n , differing from earlier expectations⁶ based partially on trends found in the broadening of ("mirror-image") alkaline-earth ions.

Transition-array-averaged semiempirical calculations⁷

have confirmed measured trends in array Stark broadening of the third row of the Periodic Table of the elements Al II to Ar II.⁸ Such array averaging becomes unsuitable when upper-state energies of some of the multiplets correspond closely ($\Delta E \ll \frac{3}{2}kT$) in energy to perturbing states connected by strong dipole transitions,^{2,3} but that is not the case here. The dashed line in Fig. 3 connects SE predictions for ns - np transition-array averages in rare-gas ions. Transition arrays perturbing the emitting levels include nd - np , ns - np , $(n+1)s$ - np , and $(n-1)d$ - np , and lower-state perturbers are also included. The computed trend line agrees closely with experimental data. It should be noticed that the experimental data of Platisa *et al.*¹⁷ were obtained at $T = 28\,300 \text{ K}$, while SE predictions are calculated at $10\,000 \text{ K}$. The Xe II linewidths of Richou *et al.*¹⁴ are obtained at 8000 K , which explains why the widths are larger than those of Nick *et al.*⁵ at $10\,000 \text{ K}$, as demonstrated in Ref. 21.

Recently, Dimitrijevic *et al.*²² demonstrated that a normalization factor can be calculated along the Ar II, Kr II, Xe II homologous sequence; their results are consistent with the present results and those of Vitel *et al.*²³

¹W. L. Wiese and N. Konjevic, *J. Quant. Spectrosc. Radiat. Transfer* **28**, 185 (1982).

²M. H. Miller, A. Lesage, and J. Puric, *Astrophys. J.* **239**, 410 (1980).

³T. L. Pittman and N. Konjevic, *J. Quant. Spectrosc. Radiat. Transfer* **35**, 247 (1986).

⁴J. Richou, S. Manola, J. L. Lebrun, and A. Lesage, *Phys. Rev. A* **29**, (1984).

⁵K. P. Nick and V. Helbig, *Phys. Scr.* **33**, 55 (1986).

⁶M. H. Miller, A. Lesage, and D. Abadie, *Phys. Rev. A* **25**, 2064 (1982).

⁷H. R. Griem, *Phys. Rev.* **165**, 258 (1968).

⁸M. H. Miller, D. Abadie, and A. Lesage, *Astrophys. J.* **291**, 219 (1985).

⁹A. Lesage, S. Sahal-Brechot, and M. H. Miller, *Phys. Rev. A* **16**, 1617 (1977).

¹⁰P. Kepple and H. R. Griem, *Phys. Rev.* **173**, 317 (1968).

¹¹V. Helbig and K. P. Nick, *J. Phys. B* **14**, 3573 (1981).

¹²J. T. Davis and J. M. Vaughan, *Astrophys. J.* **4**, 1302 (1963).

¹³H. R. Griem, *Plasma Spectroscopy* (McGraw-Hill, New York, 1964).

¹⁴V. Helbig, in *Proceedings of the Seventh International Conference on Spectral Lineshapes, Aussois, France, 1989*, edited by F. Rostas (de Gruyter, Berlin, 1985).

¹⁵P. Klein and D. Meiners, *J. Quant. Spectrosc. Radiat. Transfer* **17**, 197 (1977).

¹⁶J. M. Bridges and W. L. Wiese, *Phys. Rev.* **159**, 31 (1967).

¹⁷M. Platisa, M. S. Dimitrijevic, and N. Konjevic, *Astron. Astrophys.* **67**, 103 (1978).

¹⁸J. Chapelle, A. Sy, F. Cabannes, and J. Blandin, *J. Quant. Spectrosc. Radiat. Transfer* **8**, 1201 (1968).

¹⁹N. Konjevic, J. Labat, L. Cirkovic, and J. Puric, *Z. Phys.* **235**, 35 (1970).

²⁰J. Labat, S. Djenize, L. Cirkovic, and J. Puric, *J. Phys. B* **7**, R1174 (1974).

²¹S. Manola, N. Konjevic, J. Richou, J. L. Lebrun, and A. Lesage, *Phys. Rev. A* **38**, 5742 (1988).

²²M. S. Dimitrijevic and M. M. Popovic, *Astron. Astrophys.* (to be published).

²³Y. Vitel and M. Skowronek, *J. Phys. B* **20**, 6477 (1988); **20**, 6493 (1988).